Journal of Power Sources 192 (2009) 552–555

Contents lists available at ScienceDirect

Journal of Power Sources

journal homepage: www.elsevier.com/locate/jpowsour

Short communication

Fabrication and characterization of a cathode-supported tubular solid oxide fuel cell

Chunhua Zhao, Renzhu Liu, Shaorong Wang*, Zhenrong Wang, Jiqin Qian, Tinglian Wen

CAS Key Laboratory of Materials for Energy Conversion, Shanghai Institute of Ceramics, Chinese Academy of Sciences (SICCAS), 1295 Dingxi Road, Shanghai 200050, PR China

ARTICLE INFO

Article history:
Received 15 February 2009
Received in revised form 5 March 2009
Accepted 5 March 2009
Available online 19 March 2009

Keywords:
Tubular solid oxide fuel cell
Cathode-supported
Dip-coating
Co-sintering
Scandia-stabilized zirconia

ABSTRACT

A cathode-supported tubular solid oxide fuel cell (CTSOFC) with the length of 6.0 cm and outside diameter of 1.0 cm has been successfully fabricated via dip-coating and co-sintering techniques. A crack-free electrolyte film with a thickness of ~14 μm was obtained by co-firing of cathode/cathode active layer/electrolyte/anode at 1250 °C. The relative low densifying temperature for electrolyte was attributed to the large shrinkage of the green tubular which assisted the densification of electrolyte. The assembled cell was electrochemically characterized with humidified H_2 as fuel and O_2 as oxidant. The open circuit voltages (OCV) were 1.1, 1.08 and 1.06 V at 750, 800 and 850 °C, respectively, with the maximum power densities of 157, 272 and 358 mW cm^{-2} at corresponding temperatures.

1. Introduction

SOFC has increasing attracted interest for its high energy conversion efficiency and low impact to environment as a mean of generating electricity [1,2]. Lanthanum strontium manganites (LSM), yttria- or scandia-stabilized zirconia (YSZ or SSZ), and Ni–YSZ (SSZ) composites are the most conventional cathode, electrolyte, and anode materials, respectively [3,4]. Nowadays, planar and tubular geometric configurations are the two main SOFC designs. Compared with the planar design, the biggest advantage of tubular cells is that they are easier to seal to isolate oxidant from the fuel. Depending on the support, tubular SOFCs are divided into three categories, such as the anode-, cathode- and electrolyte-supported SOFCs. Electrode-supported tubular SOFCs possess additional advantages over electrolyte-supported cells due to the thinner electrolyte layer which can decrease the ohmic potential losses in the electrolyte. Furthermore, cathode-supported tubular solid oxide fuel cells (CTSOFCs) are particularly attractive over anode-supported ones due to their feasibility of using nickel material for current collecting for stacks. Additionally, the difficulties associated with volume contraction and expansion resulting from anode redox cycles may be avoided, since now the anode can be very thin and do not dominate the mechanical integrity of the membrane [5]. Siemens Westinghouse Power Corporation (SWPC) has successfully conducted long-term operation over 30,000 h using CTSOFCs [6].

One of the major stumbling blocks for CTSOFC commercialization is high manufacturing costs. Though LSM-supported tubular SOFC has been successfully demonstrated by SWPC, the fabrication process of thin YSZ membrane on cathode supports usually needs expensive and mass production-limited techniques (such as PVD, EVD–CVD) [5,7]. The replacement of expensive and complicated processing steps for CTSOFC components (electrolyte and electrode) by cheaper and simpler techniques has to be considered. Co-sintering is an effective way to lower the costs, but the fabrication of a dense electrolyte on a porous cathode is very difficult due to the poor chemical compatibility of cathode and electrolyte at high temperature. The reaction between LSM cathode and zirconia-based electrolyte occurs above 1200 °C [8]. But the densifying temperatures for commercial zirconia-based electrolytes are over 1300 °C [9]. The reactivity mechanism proposed by Taimatsu et al. suggests that the reaction proceeds by the unidirectional diffusion of Mn into zirconia-based oxide, and as a result, LSM at the interface becomes deficient in Mn and excess in La, leading to the formation of $La_2Zr_2O_7$ [10]. Though choosing of A-site deficient LSM can increase the co-sintering temperature, the reaction still occurs at higher temperature [8]. Liu et al. have reported the fabrication of cathode-supported SOFCs (20 mm diameter, 0.8 mm thick pellets) by using a co-sintering process; an additional $Sm_{0.2}Ce_{0.8}O_{1.95}$ layer was used between cathode and YSZ electrolyte [7]. For the cathode-supported cells, the supporting cathode dominates the

* Corresponding author. Tel.: +86 21 52411520; fax: +86 21 52411520.
E-mail address: srwang@mail.sic.ac.cn (S. Wang).

0378-7753/$ – see front matter © 2009 Elsevier B.V. All rights reserved.
doi:10.1016/j.jpowsour.2009.03.019

densification of the supported electrolyte film due to the much thicker cathode layer than the electrolyte and anode layers [3]. The acquirement of a green tubular with a large shrinkage which can assist the densification of the electrolyte film during co-sintering is significantly important to ensure the fabrication of dense electrolyte at relative low temperatures.

As a cost-effective and facile fabrication process, dip-coating followed by co-sintering has been used for the preparation of anode-supported tubular SOFCs [11]. But the fabrication of CTSOFC by this technique has not been reported. In this study, this method was developed for the fabrication of CTSOFC. The results showed that the green tubular fabricated by dip-coating has a large shrinkage and a dense electrolyte can be formed by co-sintering of cathode/cathode active layer/electrolyte/anode at 1250 °C without chemical reaction between them.

2. Experimental procedure

2.1. Synthesis of cathode powder

In order to improve the chemical compatibility between cathode and electrolyte, A-site deficient $(La_{0.8}Sr_{0.2})_{0.95}MnO_3$ (LSM95) was chosen as the cathode [8]. LSM95 powder was synthesized using the conventional solid state reaction method. Analytical grade La_2O_3, $SrCO_3$, and $MnCO_3$ were used as starting materials. A mixture of these raw materials was milled at room temperature for 2 h in a planetary mill using zirconia balls as milling medium with a small amount of ethanol as the solvent. This mixture was then calcined at 1050 °C and pure perovskite phase LSM95 was obtained.

2.2. Fabrication of a CTSOFC

Self-made LSM95 was used for preparing the cathode substrate, LSM95 and commercial $Zr_{0.89}Sc_{0.1}Ce_{0.01}O_{2-x}$ (SSZ, Daiichi Kigenso Kagaku Kogyo, Japan) with a weight ratio of 1:1 for cathode active layer (CAL), SSZ for electrolyte layer, nickel oxide (NiO, Inco Canada) powder and SSZ with a weight ratio of 1:1 for anode layer. The slurries for dip-coating process were prepared by a ball milling process that included two steps. In the first step, all the above-mentioned ceramic powders were milled in a planetary mill for 1 h using zirconia balls as milling medium with ethanol and butanone as the solvents, methyl ethyl ketone (MEK) as the disperse agent. To form sufficient porosity in the cathode substrate and CAL, 30 wt% (relative to cathode or CAL powder) graphite powder was added as pore former to the cathode and CAL slurries. Secondly, other organic additives, such as polyvinyl butyral and polyethylene glycol used as binder and plasticizer, respectively, were added, and then milled for another 2 h. Before dip-coating, the slurries were vacuum pumped for about 2 min to remove air.

The dip-coating process was carried out on a one-end-closed glass tube with an outside diameter of 12 mm. First, the LSM cathode supporting layer was dipped 5 times to reach a thickness of about 1 mm and then the CAL and electrolyte layer were dipped in turn. After drying, the green tube was rolled out from the glass tube and co-fired at 1150 °C for 4 h. Then the anode was dipped on the surface of electrolyte, waiting for co-sintering. The co-sintering temperature should be chosen to guarantee the densification of the electrolyte film, and meanwhile that no obvious reaction occurred at the interface. After checking the XRD patterns of a LSM95 and SSZ powder mixture, with the weight ratio being 1:1, and sintered at 1250 °C (such condition was more critical than the LSM95/SSZ interface of the cell, in respect of their reaction), the green tubular was heated in air to 1250 °C by a rate of 120 °C h^{-1} and co-sintered at that temperature for 4 h.

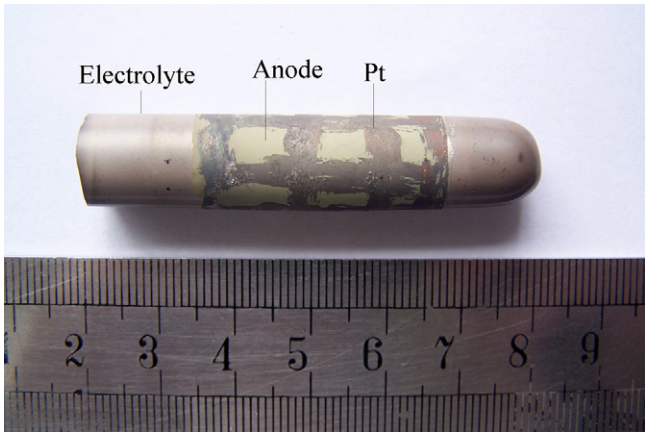

Fig. 1. The overall view of the cathode-supported tubular SOFC co-sintered at 1250 °C.

The cathode-supported tubular cell (length approximately 6.0 cm, outside diameter approximately 1.0 cm, thickness approximately 0.8–0.9 mm) was then obtained, as shown in Fig. 1. According to the anode area, the effective working area of the dipped CTSOFC was 10.1 cm^2.

2.3. Measurements

The phase composition was determined by X-ray diffraction (XRD) with Cu Kα radiation (X'pert Pro, Philips, Netherlands). The microstructure of the ceramic samples was analyzed by using a Hitachi X-600 scanning electron microscope (SEM). The cell performance and electrochemical impedance spectroscopy were measured from 750 to 850 °C with humidified H_2 (by bubbling at room temperature) as fuel and O_2 as oxidant. The flow rate of each gas was 40 ml min^{-1}. Pt paste was applied as current collector and Pt wire as lead. *I–V* curves were obtained by the volt–ampere method. The impedances were obtained using an Electrochemical Workstation IM6e (Zahner, GmbH, Germany) in the frequent range of 0.02 Hz to 20 kHz with excitation potential 20 mV. A four-probe configuration was adopted in the electrochemical testing.

3. Result and discussion

3.1. XRD analysis

The XRD pattern of the LSM95 and SSZ powder mixture is shown in Fig. 2. Clearly, the composite consists of two phases, rhombohedral perovskite-structured oxide (JCPDS: 89-4461) and tetragonal fluorite-structured oxide (JCPDS: 82-1243). No impurity phases, such as $La_2Zr_2O_7$ or $SrZrO_3$, appeared. Using XRD, Jiang et al. observed the formation of $La_2Zr_2O_7$ at the interface between $La_{0.8}Sr_{0.2}MnO_3$ and YSZ at 1150 °C [12]. It is reasonable to deduce that interface reaction between $La_{0.8}Sr_{0.2}MnO_3$ and SSZ at elevated temperature of 1250 °C can also be observed. However, with A-site deficient LSM95, the results of Fig. 2 suggest that its reaction with SSZ can be inhibited effectively to the extent of XRD limitation.

3.2. Microstructure

The typical scanning electron microscopy image of the single cell after cell testing is shown in Fig. 3. The SSZ electrolyte membrane is 14 μm in thickness and dense enough without obvious pores. The electrolyte adheres well to the CAL and anode, without any cracking or delamination after testing. It is noteworthy that the

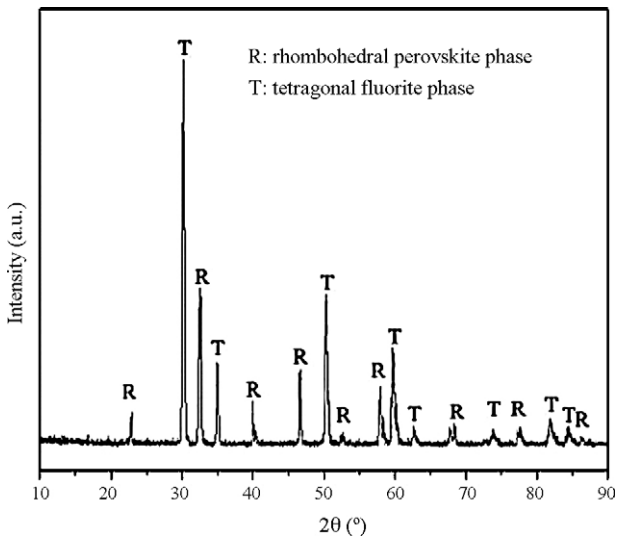

Fig. 2. XRD patterns of LSM95 and SSZ composite co-sintered at 1250 °C.

densifying temperature for electrolyte is much lower than that has been reported [9]. The relative low densifying temperature can be attributed to the large shrinkage of the green tubular which assists the densification of electrolyte [3]. The linear shrinkage of the tubular from room temperature to 1250 °C is 26%. The electrodes show typical porous microstructure. Porosity of the cathode substrate is about 34% determined by Archimedes method in water. Due to the similar microstructure of the cathode and CAL, it is hard to distinguish them directly. When it is analyzed by energy dispersive X-ray spectroscopy (not shown here), the thickness of CAL is about 65 μm.

3.3. Electrochemical performance

Fig. 4 shows the current–voltage (*I–V*) and current–power density (*I–P*) curves of the CTSOFC tested at different temperatures. The open circuit voltage (OCV) values are 1.10, 1.08 and 1.06 V at 750, 800 and 850 °C, respectively, which is in good agreement with the theoretical value calculated from the Nernst equation for each temperature [13]. The high OCV indicates that the current leakage and the gas permeation through the electrolyte layer are negligible and further confirms the prepared electrolyte is dense without any

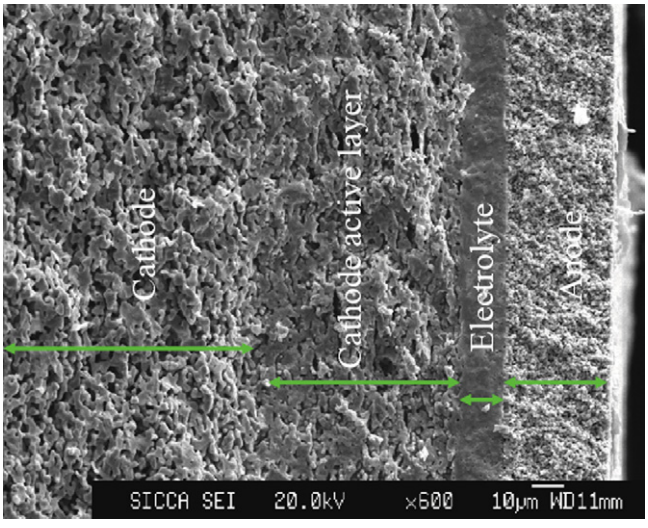

Fig. 3. SEM image of the cross-section of the CTSOFC after testing.

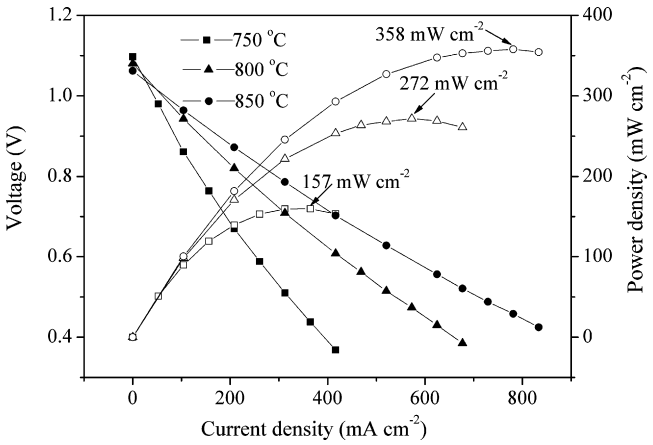

Fig. 4. *I–V* and *I–P* curves of the single cell measured at 750, 800, and 850 °C, respectively, with humidified H_2 as fuel and O_2 as oxidant. The flow rate of each gas was 40 ml min^{-1}.

cracks or defects. As seen from the *I–P* curves, peak power densities are 157, 272 and 358 mW cm^{-2} at corresponding temperatures. A maximum power density of 90 mW cm^{-2} higher than that recently reported with similar configuration measured at 800 °C [14]. The high performance of the present cell can be owed to the relative lower co-sintering temperature between cathode and electrolyte without the formation of high-resistance phase $La_2Zr_2O_7$. The other reasons may be the excellent microstructure and thin electrolyte film.

Fig. 5 shows the impedance spectroscopy measured under open circuit condition at different temperatures. The low frequency intercept corresponds to the total resistance of the cell. The high frequency intercept represents the ohmic resistance (R_o), involving ionic resistance of the electrolyte, electronic resistance of the electrodes, and some contact resistance associated with interfaces [15]. The R_o values are 0.91, 0.68, and 0.59 Ω cm^2 at 750, 800, and 850 °C, respectively. The difference between the high frequency and low frequency intercepts represents the electrode polarization resistance (R_p). The R_p values are 1.84, 0.68, and 0.43 Ω cm^2 at 750, 800, and 850 °C, respectively. The contribution of R_p to the total cell resistance, $R_p/(R_o + R_p)$, achieves 67% at 750 °C. It is well known that LSM is a typical choice as cathode material at high temperature (800–100 °C), the overpotential increases significantly below 800 °C due to the relative low reaction rate of oxygen reduction [16].

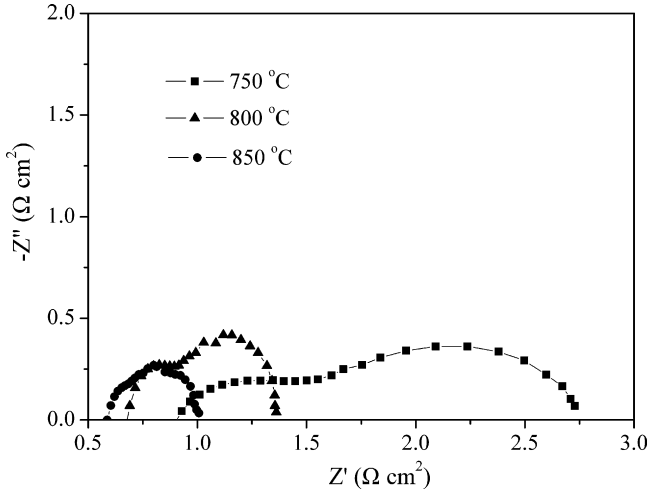

Fig. 5. Impedance spectra of the single cell measured under the open circuit state from 750 to 850 °C.

For high electrochemical performance at low temperature (below 800 °C), alterative cathode materials must be considered.

4. Conclusion

Dip-coating and co-firing processes were successfully applied to fabricate a large-size CTSOFC with the length of 6.0 cm and outside diameter of 1.0 cm. The interface reaction between cathode and electrolyte was inhibited by using A-site deficient LSM as cathode. A dense enough SSZ thin film with a thickness of ~14 μm has been obtained at 1250 °C. The maximum power densities were 157, 272 and 358 mW cm^{-2} at 750, 800 and 850 °C, respectively. To sum up, dip-coating and co-firing can be considered as a promising CTSOFC fabrication technique for future SOFC commercialization.

Acknowledgements

This work is supported by the Chinese Government High Tech Developing Project (Grant No.: 2007AA05Z151) and the Postdoctoral Foundation of China (2009).

References

[1] X.F. Ye, B. Huang, S.R. Wang, Z.R. Wang, L. Xiong, T.L. Wen, J. Power Sources 164 (2007) 203–209.
[2] T.J. Huang, M.C. Huang, J. Power Sources 168 (2007) 229–235.
[3] K. Yamahara, C.P. Jacobson, S.J. Visco, L.C.D. Jonghe, Solid State Ionics 176 (2005) 451–456.
[4] T. Yamaguchi, S. Shimizu, T. Suzuki, Y. Fujishiro, M. Awano, Mater. Lett. 62 (2008) 1518–1520.
[5] Y. Liu, S.I. Hashimoto, H. Nishino, K. Takei, M. Mori, T. Suzuki, Y. Funahashi, J. Power Sources 174 (2007) 95–102.
[6] S.C. Singhal, MRS bull. 25 (2000) 16–21.
[7] M. Liu, D. Dong, F. Zhao, J. Gao, D. Ding, X. Liu, G. Meng, J. Power Sources 182 (2008) 585–588.
[8] S.P. Jiang, J. Mater. Sci. 43 (2008) 6799–6833.
[9] Z.W. Wang, M.J. Cheng, Y.L. Dong, M. Zhang, H.M. Zhang, J. Power Sources 156 (2006) 306–310.
[10] H. Taimatsu, K. Wada, H. Kaneko, H. Yamamura, J. Am. Ceram. Soc. 75 (1992) 401–405.
[11] S. Li, S. Wang, H. Nie, T. Wen, J. Solid State Electrochem. 11 (2006) 59–64.
[12] S.P. Jiang, J.P. Zhang, Y. Ramprakash, D. Milosevic, K. Wilshier, J. Mater. Sci. 35 (2000) 2735–2741.
[13] J. Larminie, A. Dicks, Fuel Cell System Explained, 2nd ed., Wiley, New York, 2003.
[14] H. Orui, K. Watanabe, M. Arakawa, J. Power Sources 112 (2002) 90–97.
[15] C. Xia, M. Liu, Adv. Mater. 14 (2002) 521–523.
[16] Y.H. Lim, J. Lee, J.S. Yoon, C.E. Kim, H.J. Hwang, J. Power Sources 171 (2007) 79–85.